Using ultrasound and photoacoustics to monitor in situ forming implant structure and drug release

Elizabeth S.L. Berndl
Department of Physics
Ryerson University
Toronto, Canada
eberndl@ryerson.ca

Eno Hysi
Department of Physics
Ryerson University
Toronto, Canada
ehysi@ryerson.ca

Christopher Hernandez
Department of Radiology
Case Western Reserve University
Cleveland, USA
chris.hernandez@case.edu

Agata A. Exner
Department of Radiology
Case Western Reserve University
Cleveland, USA
agata.exner@case.edu

Michael C. Kolios
Department of Physics
Ryerson University
Toronto, Canada
mkolios@ryerson.ca

***Abstract*— Most chemotherapeutics (CTs) are delivered systemically, causing nausea, hair loss, fatigue and a compromised immune system. Biocompatible in situ forming implants (ISFIs) are drug delivery vehicles which are injected as a liquid before solidifying in tissues and ultimately breaking down. By dissolving CTs in an ISFI solution, they can be injected directly to the tumour site and released in a controllable manner. ISFIs can provide localized, continuous release of CT, reducing side effects. The complex phase change of ISFIs causes a variable release rate of CT. In this work, photoacoustic (PA) imaging was used for the first time to monitor a dye (mimicking CT) diffusing into a tissue mimicking phantom while quantitative ultrasound (QUS) was used to monitor the changes in the ISFI structure. ISFIs made of poly(lactic-co-glycolic acid) and Janus Green B dye dissolved in N-methyl-2-pyrrolidone in a 39:1:60 ratio were injected in tissue mimicking polyacrylamide phantoms containing titanium oxide. ISFI structure and drug release was monitored over 72 hours. At each time point, 47 planes of the phantoms were imaged using both PA (700nm) and US using the VevoLAZR system. Regions of interest within and proximal to the ISFI were selected, and average PA and QUS parameters were determined for each plane as a function of time post-implantation. This work shows the potential of PA and QUS for monitoring kinetic drug release.**

Keywords—quantitative photoacoustics, quantitative ultrasound, in situ forming implant, diffusion kinetics

I. Introduction

Chemotherapy (CT) continues to be used in the treatment of a wide variety of cancers. Because it is given systemically, side effects are also systemic, and can include fatigue, nausea, immunosuppression, loss of fertility, hair loss, and mouth sores [1]. These side effects could be drastically reduced by injecting the CT locally. A localized injection would also allow for the tumor dose to be much higher.

In situ forming implants (ISFIs) are polymers made of biodegradable poly(lactic-co-glycolic) acid (PLGA) dissolved in biocompatible and water miscible N-methyl-2-pyrrolidinone (NMP); water soluble chemicals, such as many CTs, can be dissolved in this solution. When the ISFI solution comes in contact with water, it undergoes phase inversion, rapidly forming a solid polymer outer shell and an inner cavity filled with dissolved polymer and CT. Initially, this causes a burst release of the NMP, and anything dissolved in it, which is followed by sustained release as molecules diffuse through the shell to the aqueous region [2]. Injecting CT loaded ISFI solutions directly into a tumour is therefore an appealing option to locally deliver high doses of drugs with minimum side effects [3]. There are currently two approved drugs of this type available on the market - Eligard, which carries a hormone suppressing drug, and is used primarily to treat prostate, breast and cervical cancers, and other sex-hormone disorders [4]; and Atridox, which carries an antibiotic, and is approved for use with dental implants [5]. Although there is much interest in developing ISFI products for CT, the dosage is difficult to determine because of the complex phase inversion kinetics of the polymer making the drug release rate and subsequent transport in tissue complex.

Current methods of studying diffusion from ISFIs use fluorescent dye to mimic the CT, allowing for 2-dimensional (2D) fluorescent imaging of the sample [2], [6]. However, this 2D imaging method integrates the signal over depth and therefore does not take into account the 3D CT distribution. Moreover, because the optical properties of the ISFI change as it polymerizes, the data can be difficult to interpret due to the effect of the optical property changes on the fluorescent signal detected.

In this pilot study, the ISFIs were loaded with Janus Green B dye, which acted as a substitute for CT, and were injected into scattering polyacrylamide phantoms. They were monitored at 11 or 12 different time points over the course of 72 hours using quantitative ultrasound (QUS) and photoacoustic (PA) imaging. US and PA measurements provide a 3D, non-invasive imaging method to quantitatively monitor changes in ISFI characteristics due to polymerization and diffusions rates of light absorbing molecules released from the ISFIs.

II. Material and Methods

A. *In situ porming implants and phantoms*

In situ forming implant (ISFI) solution and polyacrylamide phantoms (PAPs) were made as previously described [6], [7]. Briefly, NMP, 15.5 kDa PLGA and Janus Green B dye were

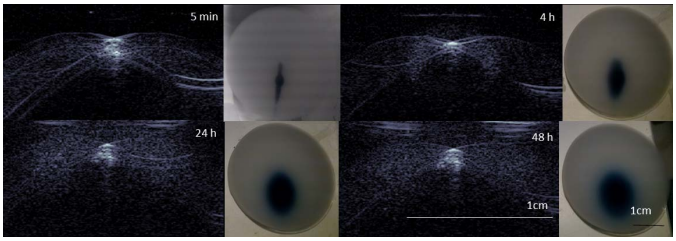

Fig. 1: Photoacoustic and optical images of an ISFI in a PAP.

978-1-5386-3383-0/17/$31.00 ©2017 IEEE

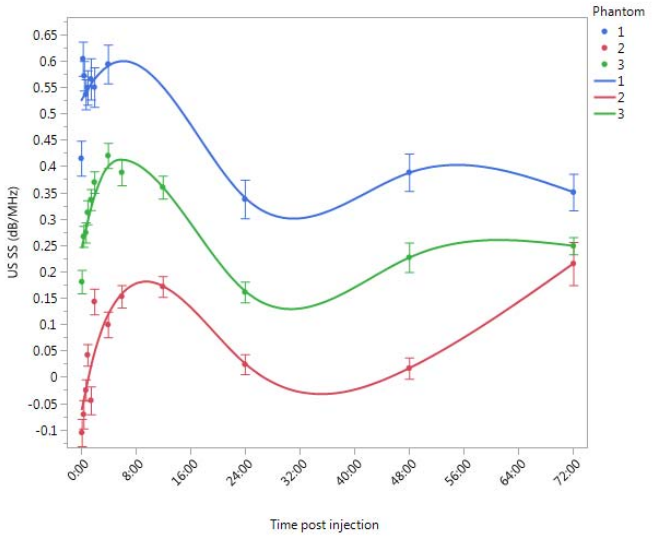

Fig. 2: Changes in ultrasound spectral slope for the ISFI in each of the three phantoms monitored during the 72 h experiment.

mixed in a 60:39:1 ratio. PAPs were made of 6.9% polyacrylamide, containing 2 mg/mL TiO, and were made in 35 mm molds. After polymerization, they were soaked for at least 24 hours in phosphate buffered saline, and then 50 µL of the ISFI solution was injected near the centre of each PAP. The PAPs were then placed in water at room temperature for the remainder of the experiment.

B. Ultrasound and photoacoustic monitoring

Data were acquired at 11 or 12 time points during a 72 hour period using a 256 element, 21 MHz central frequency linear array with the VevoLAZR system (Fujifilm-Visualsonics, Toronto, Canada). Raw radio frequency (RF) scans were taken for 47 slices over a lateral width of 10mm of each ISFI using co-registered ultrasound (US) and photoacoustics (PA) at 700nm.

C. Ultrasound and photoacoustic data processing

All RF data were processed using MATLAB (The MathWorks, Natick, MA). Within each reconstructed US B-mode image, the ISFI was manually segmented. Ten additional masks were then created by translating the segmented region between 1mm and 5mm to the left and right of the original mask (11 masks total). Quantitative ultrasound methods were used in the analysis of both the US and PA RF signals collected [8], [9]. The PA data was corrected for wavelength-dependent energy fluctuations, and the amplitude and spectral slope for both PA and US were calculated within each one of the 11 masks. The PA spectral slope methodologies have been described in previous publications of our group [10], [11]. Briefly, a 200 nm gold film was used to acquire the transducer's PA frequency response in a similar manner to which Plexiglas was used to measure the US transducer frequency response [12].

D. Statistical analysis

Statistical analysis was completed using JMP software (JMP®, Version 13. SAS Institute Inc., Cary, NC, 1989-2017.), with values of $p<0.05$ considered statistically significant. All figures show ± SEM, and use polynomial fits to show a generalized shape of the curve.

III. Results

A. Optical and photoacoustic monitoring of the phantoms

ISFIs in the PAPs were monitored regularly during the 72 hour experiment (Fig 1). As time progressed, dye leakage could be directly observed in the phantom and the beamformed photoacoustic slices of the ISFIs show a 'halo' of the PA signal spreading out from the ISFI.

B. Ultrasound spectral slope

To use ultrasound backscatter data to determine the characteristics of the ISFIs, their ultrasound spectral slopes (SS) were plotted (Fig. 2). Although the spectral slopes have different values, the plot of the SS as a function of time after implant injection have a similar shape, with a significant increase during the first four hours, a decrease at the 24 hour mark, followed by a plateau or slight increase through 72 hours.

C. Photoacoustic amplitude

The amplitude of the photoacoustic signal at various distances beyond at the ISFI show a rapid decrease for all distances during the first four hours, with significant increases in amplitude at 12 hours (0 mm translation) (Fig. 3). Signal increases are also seen after 24 hours at the 1 mm translational distance, and non-significant increases are observed after 48 hours at the 2 mm distance. The increase at 2 mm becomes significant after 72 hours, and a non-significant, increase in signal amplitude at 3 mm becomes apparent.

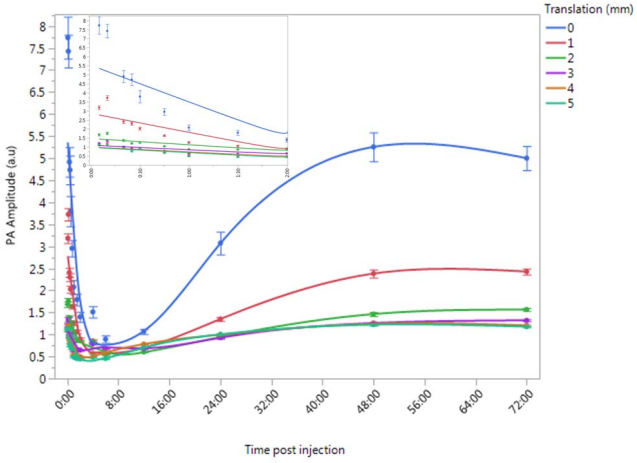

Fig. 3: PA amplitude of the ISFI and the surrounding PAP during the 72 hours post-injection. Inset: PA amplitude during the first 2 hours.

978-1-5386-3383-0/17/$31.00 ©2017 IEEE

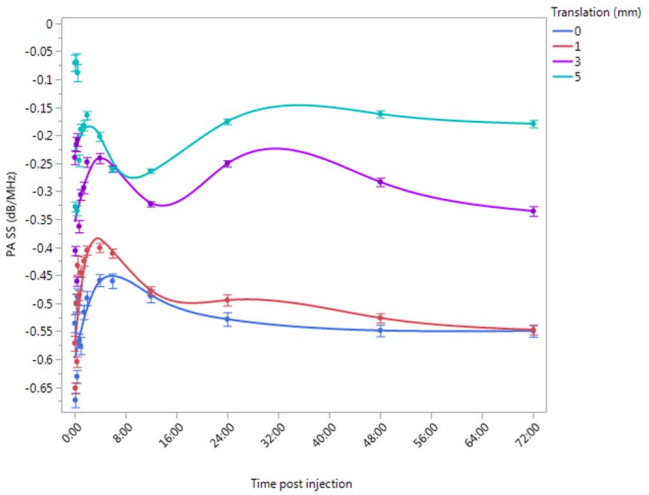

Fig. 4: Photoacoustic spectral slope in the ISFI and surrounding PAP during the 72 hour experiment. Note slopes for 2 and 4 mm translations are not shown to improve visualization.

D. Photoacoustic spectral slope

During the first four hours of the experiment, the PA SS increases in all regions measured (Fig. 4). While the ISFI (0 mm translation) peaks at -0.475 dB/MHz, and then decreases to -0.525 dB/MHz, measurements in the PAP decrease until approximately 12 hours post-injection, followed by second increase in SS. The intensity of the second increase appears to be inversely related to the distance from the ISFI, with the 1 mm shift associated with no change in SS between 12 and 24 hours, and the 3 to 5 mm shifts returning to approximately half of their initial peaks at 24 hours.

IV. Discussion

Changes in QUS spectral slope are associated with both scatterer size, and scatterer organization [13]. During the first 4 hours of the experiment, the polymerization of the ISFI solution may cause changes in the polymer organization which result in an increase of the spectral slope. As polymerization slows the rate of change of the spectral slope also decreases, suggesting a link between the ISFI structure as determined with QUS and the ISFI polymerization kinetics.

The photoacoustic amplitude in the ISFI and the surrounding PAP is highly dynamic during the first 4 hours of the experiment, showing a rapid decrease in the number of dye molecules excited by the laser within the ISFI. The change in the ISFI dye concentration was anticipated during this time period, and the time kinetic changes match the changes in the spectral slope as a function of time, indicating a large change in the polymerization of the implant.

Signals measured 5 mm away from the ISFI at early time points are likely caused by limited view, wing-like artifacts that are often observed in the presence of strong PA signals and are not representative of dye in the phantom at those locations. Such artifacts need to be accounted for in future analyses.

After the PA amplitude nadir at about 6 hours (Fig 3), PA signal intensities begin to increase, with sequential increases at the ISFI, and at regions 1, 2 and 3 mm away. The temporal changes in the PA signal amplitude correlate with the time kinetics of the observable dye diffusion in the ISFI and PAP. The data indicate that changes in PA amplitude alone may be sufficient to track diffusion of the dye in phantoms.

The PA SS is inversely proportional to effective absorber size, and is highly influenced by light fluence. Therefore, if light cannot penetrate to a particular depth, anything below that depth has a poor signal to noise ratio (SNR). Poor SNR has a strong influence on the accuracy and precision of the PA SS measurements. Because of the high dye concentration in the ISFI, it is unlikely that the light is able to penetrate through the entire implant volume. This may explain why although all regions show a peak in the measured PA SS within the first 4 hours, the PA SS in the ISFI region drops for the remainder of the experiment, while all of the regions in the PAP drop at approximately 12 hours, and then have a second peak at between 24 and 48 hours. As the PA SS is dependent on parameters that rapidly change as a function of time (e.g. density, speed of sound, and the Grüneisen parameter of the phantom) [10], [14], it is difficult to pinpoint whether specific changes in the PA SS are solely due to the changes in the effective absorber size, the absorber concentration and spatial distribution or a combination thereof.

Further work must be done to minimize the wing artifacts caused by the limited view of the linear array transducer, which are particularly evident in the PA amplitude (Fig 1). Possible solutions include using suppressing such artifacts using more sophisticated reconstruction algorithms [15] or avoiding the artifacts using the tomographic approaches based on circular arrays (e.g. iThera MSOT system). Finally, further data must be collected where the ISFIs are formed ex vivo in tissue rather than in PAPs. The increased complexity of tissue is important to understand before attempting monitoring in vivo.

V. Conclusions

Quantitative ultrasound can be used to characterize changes in an ISFI as it undergoes phase inversion in a polyacrylamide phantom, providing insight into the time kinetics of the structural changes in the ISFI. Changes in the concentration of an absorbing dye in a polyacrylamide phantom can be monitored using PA imaging. QUS and PA methods therefore can be used as a non-invasive method of monitoring diffusion of optical absorbers, such as chemotherapeutics, from an ISFI providing more comprehensive 3D data than previously utilized methods.

Acknowledgements

This work is supported by the Terry Fox New Frontiers Program Project Grant in Ultrasound and MRI for Cancer Therapy (CIHR#TFF 105267). This research was undertaken, in part, thanks to funding from the Canada Research Chairs Program awarded to M.C.K. E. H. is supported through an NSERC Canada Vanier Graduate Scholarship. This research project was supported by grants from the National Institute of Biomedical Imaging and Bioengineering (R01EB016960) awarded to A.A.E. Funding to purchase the equipment was provided by the Canada Foundation for Innovation, the Ontario Ministry of Research and Innovation, and Ryerson University.

978-1-5386-3383-0/17/$31.00 ©2017 IEEE

References

[1] "Chemotherapy Side Effects." [Online]. Available: https://www.cancer.org/treatment/treatments-and-side-effects/treatment-types/chemotherapy/chemotherapy-side-effects.html. [Accessed: 21-Aug-2017].

[2] L. Solorio, B. M. Babin, R. B. Patel, J. Mach, N. Azar, and A. A. Exner, "Noninvasive characterization of in situ forming implants using diagnostic ultrasound," J. Controlled Release, vol. 143, no. 2, pp. 183–190, Apr. 2010.

[3] A. Hatefi and B. Amsden, "Biodegradable injectable in situ forming drug delivery systems," J. Controlled Release, vol. 80, no. 1–3, pp. 9–28, 2002.

[4] O. Sartor, "Eligard: leuprolide acetate in a novel sustained-release delivery system," Urology, vol. 61, no. 2, pp. 25–31, 2003.

[5] A. Buchter, J. Kleinheinz, U. Meyer, and U. Joos, "Treatment of severe peri-implant bone loss using autogenous bone and a bioabsorbable polymer that delivered doxycycline (Atridox(TM))," Br. J. Oral Maxillofac. Surg., vol. 42, no. 5, pp. 454–456, 2004.

[6] L. Solorio, A. M. Olear, H. Zhou, A. C. Beiswenger, and A. A. Exner, "Effect of cargo properties on in situ forming implant behavior determined by noninvasive ultrasound imaging," Drug Deliv. Transl. Res., vol. 2, no. 1, pp. 45–55, Feb. 2012.

[7] J. Stukel, M. Goss, H. Zhou, W. Zhou, R. Willits, and A. A. Exner, "Development of a High-Throughput Ultrasound Technique for the Analysis of Tissue Engineering Constructs," Ann. Biomed. Eng., vol. 44, no. 3, pp. 793–802, Mar. 2016.

[8] R. M. Vlad, G. J. Czarnota, A. Giles, M. D. Sherar, J. W. Hunt, and M. C. Kolios, "High-frequency ultrasound for monitoring changes in liver tissue during preservation," Phys. Med. Biol., vol. 50, no. 2, p. 197, 2005.

[9] R. M. Vlad, M. C. Kolios, and G. J. Czarnota, "Ultrasound imaging of apoptosis: spectroscopic detection of DNA-damage effects at high and low frequencies," Methods Mol. Biol. Clifton NJ, vol. 682, pp. 165–187, 2011.

[10] E. Hysi, R. K. Saha, and M. C. Kolios, "Photoacoustic ultrasound spectroscopy for assessing red blood cell aggregation and oxygenation," J. Biomed. Opt., vol. 17, no. 12, p. 125006, Dec. 2012.

[11] E. Hysi, L. A. Wirtzfeld, J. P. May, E. Undzys, S.-D. Li, and M. C. Kolios, "Photoacoustic signal characterization of cancer treatment response: Correlation with changes in tumor oxygenation," Photoacoustics, vol. 5, pp. 25–35, Mar. 2017.

[12] L. A. Wirtzfeld et al., "Cross-Imaging Platform Comparison of Ultrasonic Backscatter Coefficient Measurements of Live Rat Tumors," J. Ultrasound Med., vol. 29, no. 7, pp. 1117–1123, Jul. 2010.

[13] R. K. Saha and M. C. Kolios, "Effects of cell spatial organization and size distribution on ultrasound backscattering," IEEE Trans. Ultrason. Ferroelectr. Freq. Control, vol. 58, no. 10, pp. 2118–2131, Oct. 2011.

[14] E. Hysi, E. M. Strohm, and M. C. Kolios, "Probing Different Biological Length Scales Using Photoacoustics: From 1 To 1000 MHz," in Handbook of Photonics for Biomedical Engineering, A. H.-P. Ho, D. Kim, and M. G. Somekh, Eds. Springer Netherlands, 2014, pp. 1–18.

[15] S. Ma, S. Yang, and H. Guo, "Limited-view photoacoustic imaging based on linear-array detection and filtered mean-backprojection-iterative reconstruction," J. Appl. Phys., vol. 106, no. 12, p. 123104, Dec. 2009.

978-1-5386-3383-0/17/$31.00 ©2017 IEEE